Power spectrum of light scattered by a two-level atom in the presence of a pulse-train driving field

Mark A. Newbold and Gregory J. Salamo
Department of Physics, University of Arkansas, Fayetteville, Arkansas 72701
(Received 31 January 1980)

The power spectrum of the light scattered by a two-level atom in the presence of a coherent continuous-pulse-train driving field is analyzed. Separate expressions for the coherent and incoherent components of the spectrum are obtained. The coherent part of the spectrum consists of a series of spikes (delta functions) which are displaced from the optical carrier by multiples of the pulse repetition frequency. The incoherent spectrum can have fixed peaks at these same frequencies plus sidebands equally spaced on opposite sides of these fixed peaks. That is, the spectrum consists of a series of triplets. The special case of a two-mode driving field is treated numerically and graphs of spectra are presented.

I. INTRODUCTION

The spectrum of light scattered from a strongly driven two-level atom has received much attention recently.[1] The experiments of Wu, Grove, and Ezekiel[2] support the predictions of the theory presented by Mollow.[3] In Mollow's work it is assumed that the atom is driven by a perfectly monochromatic optical field. It is the purpose of the present paper to extend Mollow's work to the case of a pulse-train driving field such as that produced by a mode-locked cw dye laser. As in the Mollow theory, it is assumed that the atom has come to equilibrium with the driving field through radiation damping.

II. THE THEORETICAL MODEL

Following Ref. 3, we consider a single atom fixed at the coordinate origin and driven by a near-resonant classical[4] optical field. The atom fluoresces through its interaction with a bath of quantum field oscillators. It is assumed that only two atomic levels are involved in the interaction: $|0\rangle$ and $|1\rangle$, having energies 0 and $\hbar\omega_0$, respectively. The following atomic operators may be defined at $t=0$ in the Heisenberg picture:

$$a(0)=|0\rangle\langle 1| \tag{1a}$$

and

$$a^\dagger(0)=|1\rangle\langle 0|\,. \tag{1b}$$

The electric field operator may be decomposed into its positive and negative frequency parts:

$$\vec{\mathbf{E}}(\vec{\mathbf{r}},t)=(1/\sqrt{2})[\vec{\mathbf{E}}^{(+)}(\vec{\mathbf{r}},t)+\vec{\mathbf{E}}^{(-)}(\vec{\mathbf{r}},t)]\,, \tag{2}$$

where

$$\vec{\mathbf{E}}^{(+)}(\vec{\mathbf{r}},t)=\epsilon(\vec{\mathbf{r}},t)\hat{e}_0+i\sum_{\vec{k},s}(\hbar\omega_{\vec{k}}/V)^{1/2}\hat{e}_{\vec{k},s}b_{\vec{k},s}(t)e^{i\vec{k}\cdot\vec{r}} \tag{3}$$

and $\vec{\mathbf{E}}^{(-)}(\vec{\mathbf{r}},t)$ is given by the adjoint of (3). Here $b_{\vec{k},s}$ is the annihilation operator for the quantized-field mode with wave vector $\vec{k}$ and polarization index $s(=1,2)$, $\omega_{\vec{k}}$ is its frequency, $\hat{e}_{\vec{k},s}$ is its polarization vector, and V is the quantization volume; $\epsilon(\vec{\mathbf{r}},t)$ represents the positive frequency part of the classical electric field, with polarization vector $\hat{e}_0$. Near resonance, the dipole interaction Hamiltonian may be approximated by

$$H_I(t)=-(1/\sqrt{2})[a^\dagger(t)\vec{\mu}\cdot\vec{\mathbf{E}}^{(+)}(0,t)+a(t)\vec{\mu}^*\cdot\vec{\mathbf{E}}^{(-)}(0,t)]\,, \tag{4}$$

where $\vec{\mu}\equiv\langle 1|\vec{\mathbf{d}}|0\rangle$, with $\vec{\mathbf{d}}$ being the atomic-dipole-moment operator (at $t=0$ in the Heisenberg picture). We write, for the positive frequency part of the classical driving field,

$$\epsilon(0,t)=[\epsilon_1(t)-i\epsilon_2(t)]\mathcal{E}e^{-i\omega t}/\sqrt{2}(\vec{\mu}\cdot\hat{e}_0)\,, \tag{5}$$

where ω is the optical carrier frequency, $\epsilon_1(t)$ and $\epsilon_2(t)$ are real quantities representing the field envelope at the position of the atom, and the time-independent factors have been inserted for later convenience. In Ref. 3 (Eq. 3.16), the classical driving field was assumed to be perfectly monochromatic (ϵ_1 and ϵ_2 constant). In the present paper, we generalize this work by assuming that the driving field is that of a pulse train. Thus ϵ_1 and ϵ_2 are assumed to be repetitive with period τ_r:

$$\epsilon_1(t+\tau_r)=\epsilon_1(t)\,, \tag{6a}$$

$$\epsilon_2(t+\tau_r)=\epsilon_2(t)\,. \tag{6b}$$

As discussed in Ref. 3, the positive-frequency part of the scattered field is given approximately by

$$\vec{\mathbf{E}}^{(+)}(\vec{\mathbf{r}},t)=\vec{\phi}(\vec{\mathbf{r}})a(t-r/c)+\vec{\mathbf{E}}_F^{(+)}(\vec{\mathbf{r}},t)\,, \tag{7}$$

where

$$\vec{\phi}(\vec{\mathbf{r}})\equiv(\omega_0^2/2\sqrt{2}\pi c^2r^3)\vec{\mathbf{r}}\times(\vec{\mu}\times\vec{\mathbf{r}}) \tag{8}$$

and $\vec{\mathbf{E}}_F(\vec{\mathbf{r}},t)$ is the "freely-propagating part" of the electric-field operator—a linear combination of

 © 1980 The American Physical Society

annihilation operators $b_{\vec{k},s}(0)$.

In Ref. 3, the following expression is evaluated:

$$I(\nu,\vec{r})\equiv\int_{-\infty}^{\infty}d\tau\langle\vec{E}^{(-)}(\vec{r},t)\cdot\vec{E}^{(+)}(\vec{r},t+\tau)\rangle e^{i\nu\tau}.$$

This quantity is interpreted as the power spectrum of the scattered light. In the analysis of Ref. 3, this expression is independent of t because the atom is in equilibrium with a monochromatic driving field. In the present paper however, we assume equilibrium with a pulse-train driving field.[5] As will be seen below, the second-order field correlation function $\langle\vec{E}^{(-)}(\vec{r},t)\cdot\vec{E}^{(+)}(\vec{r},t+\tau)\rangle$ now has a periodic t dependence, with the same period as the pulse repetition time. It might at first seem natural to proceed with the above definition of the power spectrum, allowing the spectrum to be t dependent. However, this would not be consistent with the frequency-time uncertainty relation. In order to resolve features narrower than the repetition frequency, a real detector must sample over many periods. Thus its output would not vary significantly over a single period. The above-defined quantity therefore does not represent the response of a real detector.

A calculation of the response of a high-resolution Fabry-Perot interferometer to a narrow-bandwidth classical input field with a periodic envelope suggests that the observable power spectrum is given by the following t-averaged expression

$$I(\nu,\vec{r})\equiv\frac{1}{\tau_r}\int_0^{\tau_r}dt\int_{-\infty}^{\infty}d\tau\langle\vec{E}^{(-)}(\vec{r},t)\cdot\vec{E}^{(+)}(\vec{r},t+\tau)\rangle e^{i\nu\tau}. \tag{9}$$

Any reasonable definition of the power spectrum must satisfy certain requirements—it must reduce to Mollow's definition in the special case that the field correlation function is independent of t; it must be time independent; and it must be everywhere real and positive. Equation (9) clearly satisfies the first two requirements. To see that the third requirement is also satisfied one may replace τ by $\tau-t$, extend the t averaging to $\pm\infty$, and bring the integrations inside the expectation-value brackets. The resulting expression is the expectation value of a positive operator and is thus necessarily real and positive. In this paper, we take Eq. (9) to represent the power spectrum of the scattered light when the driving field is that of a pulse train.

Using (7) and (9) and assuming that $\vec{E}_F(\vec{r},t)$ does not contribute to the field correlation function, we obtain

$$I(\nu,\vec{r})=|\vec{\phi}(\vec{r})|^2\tilde{g}(\nu), \tag{10}$$

where

$$\tilde{g}(\nu)\equiv\frac{1}{\tau_r}\int_0^{\tau_r}dt\int_{-\infty}^{\infty}d\tau\langle a^\dagger(t)a(t+\tau)\rangle e^{i\nu\tau}. \tag{11}$$

The quantity $\tilde{g}(\nu)$ contains the frequency dependence of the power spectrum and its evaluation is therefore our primary concern in the remainder of this paper.

III. THE BLOCH EQUATIONS

It is shown in Ref. 3 on the basis of a Markoff approximation that two-time atomic expectation values such as the atomic correlation function in Eq. (11) may be obtained directly from the solutions to the equations governing the evolution of the single-time expectation values, α, α^*, $\bar{n}$, and $\bar{m}$, defined in Ref. 3 by

$$\alpha(t)=\langle a(t)\rangle, \tag{12a}$$

$$\alpha^*(t)=\langle a^\dagger(t)\rangle, \tag{12b}$$

$$\bar{n}(t)=\langle a^\dagger(t)a(t)\rangle, \tag{12c}$$

$$\bar{m}(t)=\langle a(t)a^\dagger(t)\rangle. \tag{12d}$$

We find it convenient to transform from the above variables to real atomic variables u, v, w, and x:

$$\begin{bmatrix}u(t)\\v(t)\\w(t)\\x\end{bmatrix}=\begin{bmatrix}e^{i\omega t}&e^{-i\omega t}&0&0\\ie^{i\omega t}&-ie^{-i\omega t}&0&0\\0&0&1&-1\\0&0&1&1\end{bmatrix}\begin{bmatrix}\alpha(t)\\\alpha^*(t)\\\bar{n}(t)\\\bar{m}(t)\end{bmatrix}. \tag{13}$$

Applying the same change of variables to the equations of motion [Ref. 3, Eqs. (3.13)] one obtains the Bloch equations[6]:

$$\frac{d}{dt}\begin{bmatrix}u(t)\\v(t)\\w(t)\\x\end{bmatrix}=\begin{bmatrix}-\frac{1}{2}\kappa&-\Delta\omega&-\epsilon_2(t)&0\\\Delta\omega&-\frac{1}{2}\kappa&\epsilon_1(t)&0\\\epsilon_2(t)&-\epsilon_1(t)&-\kappa&-\kappa\\0&0&0&0\end{bmatrix}\begin{bmatrix}u(t)\\v(t)\\w(t)\\x\end{bmatrix}. \tag{14}$$

Here $\Delta\omega$ is the off-resonance parameter for the atom

$$\Delta\omega=\omega_0-\omega \tag{15}$$

and κ is the radiative relaxation rate (inverse lifetime)

$$\kappa=|\vec{\mu}|^2\omega_0^3/3\pi\hbar c^3. \tag{16}$$

The general solution to the first-order linear coupled equations (14) at a time t_2 is related to the solution at another time t_1 by a linear transformation:

$$\begin{bmatrix} u(t_2) \\ v(t_2) \\ w(t_2) \\ x \end{bmatrix} = \underline{T}(t_2, t_1) \begin{bmatrix} u(t_1) \\ v(t_1) \\ w(t_1) \\ x \end{bmatrix}, \tag{17}$$

where $\underline{T}(t_2, t_1)$ is a 4×4 matrix. Unfortunately, with $\kappa \neq 0$, the matrix function $\underline{T}(t_2, t_1)$ cannot be expressed analytically except in the special case, treated by Mollow, of a monochromatic driving field (ϵ_1 and ϵ_2 constant). However, insight into the structure of the power spectrum can be gained by treating $\underline{T}(t_2, t_1)$ symbolically. For comparison between theory and experiment, $\underline{T}(t_2, t_1)$ can be readily obtained by numerically integrating the Bloch equations.[7] Some of the properties of $\underline{T}(t_2, t_1)$ follow

(i) $\underline{T}(t_2, t_1)$ has the group property:

$$\underline{T}(t_3, t_1) = \underline{T}(t_3, t_2)\underline{T}(t_2, t_1). \tag{18}$$

(ii) As a consequence of Eqs. (6), $\underline{T}(t_2, t_1)$ is periodic in the following sense:

$$\underline{T}(t_2 + \tau_r, t_1 + \tau_r) = \underline{T}(t_2, t_1). \tag{19}$$

(iii) Since x is constant in the Bloch equations, the fourth row of $\underline{T}(t_2, t_1)$ has a very simple form

$$[\underline{T}(t_2, t_1)]_{4i} = \begin{cases} 0, & i = 1, 2, 3 \\ 1, & i = 4. \end{cases} \tag{20}$$

(iv) It is easy to show using Eqs. (14) that for $t_2 \geq t_1$ and $x = 0$,

$$[u^2(t_2) + v^2(t_2) + w^2(t_2)] \leq e^{-\kappa(t_2 - t_1)}[u^2(t_1) + v^2(t_1) + w^2(t_1)]. \tag{21}$$

That is, a solution with $x = 0$ decays away in a time comparable to the atomic relaxation time. This may be translated into a statement about some of the elements of $\underline{T}(t_2, t_1)$. We define a 3×3 submatrix $\underline{T}_3(t_2, t_1)$:

$$[\underline{T}_3(t_2, t_1)]_{ij} \equiv [\underline{T}(t_2, t_1)]_{ij}, \quad i, j = 1, 2, 3. \tag{22}$$

Equation (21) implies that for $t_2 \geq t_1$,

$$|\underline{T}_3(t_2, t_1)\vec{p}| \leq e^{-\kappa(t_2 - t_1)/2} |\vec{p}|, \tag{23}$$

where $\vec{p}$ is any 3×1 column vector and the bars indicate the length (norm) of the vector.

Though the driving field envelope is periodic (Eqs. 6), the general solution to Eqs. (14) is not periodic. For example, as noted above any solution with $x = 0$ decays to zero as $t \to \infty$. However, solutions representing a physical atomic state, as defined by Eqs. (12) and (13), must have $x = \langle a^\dagger a + a a^\dagger \rangle = 1$. In this subset of solutions, there is a unique periodic solution—the "equilibrium Bloch vector,"[5] with components $u_e(t)$, $v_e(t)$, and $w_e(t)$ defined by

$$\underline{T}(t + \tau_r, t) \begin{bmatrix} u_e(t) \\ v_e(t) \\ w_e(t) \\ 1 \end{bmatrix} = \begin{bmatrix} u_e(t) \\ v_e(t) \\ w_e(t) \\ 1 \end{bmatrix}. \tag{24}$$

Using (20) and noting that as a consequence of (23) the 3×3 matrix $\underline{I}_3 - \underline{T}_3(t + \tau_r, t)$ (where $\underline{I}_3$ is the 3×3 identity matrix) is invertible, the equilibrium Bloch vector is easily obtained:

$$\begin{bmatrix} u_e(t) \\ v_e(t) \\ w_e(t) \end{bmatrix} = [\underline{I}_3 - \underline{T}_3(t + \tau_r, t)]^{-1} \begin{bmatrix} [\underline{T}(t + \tau_r, t)]_{14} \\ [\underline{T}(t + \tau_r, t)]_{24} \\ [\underline{T}(t + \tau_r, t)]_{34} \end{bmatrix}. \tag{25}$$

Any solution to the Bloch equations (14) representing a physical atomic state (i.e., having $x = 1$) decays to this equilibrium solution within several atomic relaxation times. This follows from Eq. (21) since the difference between the given solution and the $x = 1$ equilibrium solution is itself an $x = 0$ solution to Eq. (14). Thus the difference decays to zero according to (21) and the atom comes to a periodic equilibrium.

IV. THE POWER SPECTRUM

A. The power spectrum in terms of the Bloch equations

In Ref. 3 (Eq. 4.6) an expression for the atomic correlation function is obtained via a "quantum regression theorem." Transforming this expression to our representation using Eqs. (13) one obtains (see Appendix)

$$\langle a^\dagger(t) a(t + \tau) \rangle = \tfrac{1}{4} e^{-i\omega\tau}(1, -i, 0, 0)\underline{T}(t + \tau, t)\underline{M} \begin{bmatrix} u_e(t) \\ v_e(t) \\ w_e(t) \\ 1 \end{bmatrix} \tag{26}$$

for $\tau \geq 0$, where we define

$$\underline{M} \equiv \begin{bmatrix} 0 & 0 & 1 & 1 \\ 0 & 0 & i & i \\ -1 & -i & 0 & 0 \\ 1 & i & 0 & 0 \end{bmatrix}, \tag{27}$$

and $(1, -i, 0, 0)$ is a 1×4 row matrix. It is as-

sumed in writing (26) that the atom is in equilibrium with the driving field at time t. Referring to (19), (17), and (24) one can see that the atomic correlation function given by (26) is periodic in t:

$$\langle a^\dagger(t+\tau_r)a(t+\tau_r+\tau)\rangle = \langle a^\dagger(t)a(t+\tau)\rangle . \tag{28}$$

Using (28) and noting that $\langle a^\dagger(t)a(t')\rangle = \langle a^\dagger(t')a(t)\rangle^*$, we can rewrite Eq. (11) as

$$\tilde{g}(\nu) = \frac{2}{\tau_r}\,\mathrm{Re}\int_0^{\tau_r} dt \int_0^\infty d\tau \langle a^\dagger(t)a(t+\tau)\rangle e^{i\nu\tau}, \tag{29}$$

where Re denotes the real part. If we now insert (26) into (29) we obtain

$$\tilde{g}(\nu') = \frac{1}{2\tau_r}\,\mathrm{Re}\int_0^{\tau_r} dt \int_0^\infty d\tau\, e^{i\nu'\tau}(1,-i,0,0) \times \underline{T}(t+\tau,t)\underline{M}\begin{bmatrix} u_e(t) \\ v_e(t) \\ w_e(t) \\ 1 \end{bmatrix} \tag{30}$$

where frequencies are now measured relative to the carrier frequency ω:

$$\nu' \equiv \nu - \omega . \tag{31}$$

B. Separation of the coherent and incoherent parts of the power spectrum

The τ integral in (30) may be written as an infinite sum of cycle integrals:

$$\int_0^\infty e^{i\nu'\tau}\underline{T}(t+\tau,t)d\tau = \sum_{n=0}^\infty \int_{n\tau_r}^{(n+1)\tau_r} e^{i\nu'\tau}\underline{T}(t+\tau,t)d\tau = \sum_{n=0}^\infty \int_0^{\tau_r} \underline{T}(t+\tau,0)[\underline{T}(\tau_r,0)]^n\underline{T}(0,t)e^{i\nu'(\tau+n\tau_r)}d\tau ,$$

where Eqs. (18) and (19) were used in the last step. Thus we can write $\tilde{g}(\nu')$ as

$$\tilde{g}(\nu') = \frac{1}{2\tau_r}\,\mathrm{Re}\int_0^{\tau_r} d\tau \int_0^{\tau_r} dt\, e^{i\nu'\tau}(1,-i,0,0)\underline{T}(t+\tau,0)\underline{S}(\nu')\underline{T}(0,t)\underline{M}\begin{bmatrix} u_e(t) \\ v_e(t) \\ w_e(t) \\ 1 \end{bmatrix}, \tag{32}$$

where

$$\underline{S}(\nu') = \sum_{n=0}^\infty [\underline{T}(\tau_r,0)]^n e^{i\nu' n\tau_r} . \tag{33}$$

Since $\underline{T}(\tau_r,0)$ has an eigenvector with unit eigenvalue (the equilibrium Bloch vector defined by Eq. (24) with $t=0$), part of $[\underline{T}(\tau_r,0)]^n$ persists as $n\to\infty$.[8] This means that the quantity which is being Fourier transformed in Eq. (30) has a repetitive component, so the power spectrum is expected to include Dirac delta functions. It is desirable to separate the part of the spectrum composed of delta functions from the continuous part. With this goal in mind, we introduce a projection matrix $\underline{P}$ defined as the part of $[\underline{T}(\tau_r,0)]^n$ which persists as $n\to\infty$:

$$\underline{P} \equiv \lim_{n\to\infty}[\underline{T}(\tau_r,0)]^n . \tag{34}$$

The existence of this limit is apparent from Eqs. (21) and (24). Explicitly, we can write

$$\underline{P} = \begin{bmatrix} u_e(0) \\ v_e(0) \\ w_e(0) \\ 1 \end{bmatrix}(0,0,0,1) . \tag{35}$$

Clearly $\underline{P}$ is a projection matrix ($\underline{P}^2 = \underline{P}$). The definition (34) implies that

$$\underline{T}(\tau_r,0)\underline{P} = \underline{P} \tag{36}$$

and

$$\lim_{n\to\infty}[\underline{T}(\tau_r,0)]^n(\underline{I}-\underline{P}) = 0 . \tag{37}$$

Thus $\underline{P}$ may be used to project the part of $[\underline{T}(\tau_r,0)]^n$ which persists as $n\to\infty$ in (33). By replacing $\underline{S}(\nu')$ in Eq. (32) by $\underline{S}(\nu')\underline{P}+\underline{S}(\nu')[\underline{I}-\underline{P}]$, we can separate the spectrum into two parts:

$$\tilde{g}(\nu') = \tilde{g}_{\mathrm{coh}}(\nu') + \tilde{g}_{\mathrm{inc}}(\nu') , \tag{38}$$

where

$$\tilde{g}_{\mathrm{coh}}(\nu') \equiv \frac{1}{2\tau_r}\,\mathrm{Re}\int_0^{\tau_r} d\tau \int_0^{\tau_r} dt\, e^{i\nu'\tau}(1,-i,0,0)\underline{T}(t+\tau,0)\underline{S}(\nu')\underline{P}\underline{T}(0,t)\underline{M}\begin{bmatrix} u_e(t) \\ v_e(t) \\ w_e(t) \\ 1 \end{bmatrix} \tag{39}$$

and

$$\tilde{g}_{\rm inc}(\nu')\equiv\frac{1}{2\tau_r}\,\mathrm{Re}\int_0^{\tau_r}d\tau\int_0^{\tau_r}dt\,e^{i\nu'\tau}(1,-i,0,0)\underline{T}(t+\tau,0)\underline{S}(\nu')[\underline{I}-\underline{P}]\underline{T}(0,t)\underline{M}\begin{bmatrix}u_e(t)\\v_e(t)\\w_e(t)\\1\end{bmatrix}. \tag{40}$$

The subscripts anticipate the result that $\tilde{g}_{\rm coh}$ and $\tilde{g}_{\rm inc}$ are, respectively, the coherent and incoherent components of the power spectrum. We now examine each of these components separately.

C. Reduction of the coherent component of the power spectrum

Using Eq. (33) and (36) we can write

$$\underline{S}(\nu')\underline{P}=\underline{P}\sum_{n=0}^{\infty}e^{i\nu' n\tau_r}. \tag{41}$$

Hence one can write $\tilde{g}_{\rm coh}(\nu')$ as

$$\tilde{g}_{\rm coh}(\nu')=\mathrm{Re}\sum_{n=0}^{\infty}e^{i\nu' n\tau_r}\int_0^{\tau_r}f(\tau)e^{i\nu'\tau}d\tau, \tag{42}$$

where

$$f(\tau)\equiv\frac{1}{2\tau_r}\int_0^{\tau_r}(1,-i,0,0)\underline{T}(t+\tau,0)\underline{P}\underline{T}(0,t')\underline{M}\begin{bmatrix}u_e(t)\\v_e(t)\\w_e(t)\\1\end{bmatrix}dt. \tag{43}$$

Equation (43) reduces, with the help of (35), (17), (20), and (27) to

$$f(\tau)=\frac{1}{2\tau_r}\int_0^{\tau_r}[u_e(t+\tau)-iv_e(t+\tau)]\times[(u_e(t)+iv_e(t)]dt. \tag{44}$$

Due to the periodicity of u_e and v_e, $f(\tau)$ is itself periodic and one can show using (44) that

$$\int_0^{\tau_r}f(\tau)e^{i\nu'(\tau-\tau_r/2)}d\tau$$

is real. The right-hand side of Eq. (42) can therefore be written as the product of the above expression and

$$\mathrm{Re}\sum_{n=0}^{\infty}e^{i\nu' n\tau_r}e^{i\nu'\tau_r/2}=\tfrac{1}{2}\sum_{n=-\infty}^{\infty}e^{i\nu'(n+1/2)\tau_r}=\frac{\pi}{\tau_r}\sum_{m=-\infty}^{\infty}\delta\left(\nu'-\frac{2m\pi}{\tau_r}\right)e^{i\nu'\tau_r/2},$$

where the Dirac delta function appears in the last step. Therefore Eq. (42) reduces [using (44) and replacing τ by $\tau-t$] to

$$\tilde{g}_{\rm coh}(\nu')=\sum_{m=-\infty}^{\infty}a_{\rm coh}(m)\delta\left(\nu'-\frac{2m\pi}{\tau_r}\right), \tag{45}$$

where we define

$$a_{\rm coh}(m)\equiv\frac{\pi}{2}\left|\frac{1}{\tau_r}\int_0^{\tau_r}e^{i2m_\pi\tau/\tau_r}[u_e(\tau)-iv_e(\tau)]d\tau\right|^2. \tag{46}$$

This component of the scattered light is due to the semiclassical dipole moment of the atom and we therefore refer to it as the "coherent" part. Equation (45) shows that the coherent spectrum consists of a series of spikes displaced from the optical carrier by multiples of the cycle frequency $2\pi/\tau_r$. The presence of these spikes is due to the periodicity of the semiclassical dipole moment at equilibrium. We note that in the special case, treated by Mollow, of a monochromatic driving field, u_e-iv_e oscillates harmonically and the coherent spectrum consists of a single elastic spike at the frequency of the driving field. It will be seen in Sec. VI that in the more general case, the spectral profile of the coherently scattered energy is different from that of the driving field—the coherent scattering with a pulse-train driving field is not in general elastic.

D. Reduction of the incoherent component of the power spectrum

We can rewrite Eq. (33) as

$$\underline{S}(\nu')=\lim_{N\to\infty}\underline{S}_N(\nu'), \tag{47}$$

where

$$\underline{S}_N(\nu')\equiv\sum_{n=0}^{N}[\underline{T}(\tau_r,0)]^n e^{i\nu' n\tau_r}. \tag{48}$$

Using Eq. (48) one can obtain the following identity:

$$\underline{S}_N(\nu')[\underline{I}-\underline{T}(\tau_r,0)e^{i\nu'\tau_r}]=\underline{I}-[\underline{T}(\tau_r,0)]^{(N+1)}e^{i\nu'(N+1)\tau_r}. \tag{49}$$

We define a 4×4 matrix $\underline{K}(\nu')$ as follows:

$$[\underline{K}(\nu')]_{ij}=\begin{cases}[\underline{I}_3-\underline{T}_3(\tau_r,0)e^{i\nu'\tau_r}]^{-1}_{ij} & i,j=1,2,3\\ 0 & \text{otherwise}\end{cases} \tag{50}$$

and note that due to (35),

$$\underline{P}\underline{K}(\nu')=0. \tag{51}$$

Multiplying (49) from the right by $\underline{K}(\nu')[\underline{I}-\underline{P}]$ and using (22) and (35) we obtain

$$\underline{S}_N(\nu')[\underline{I}-\underline{P}]=\underline{K}(\nu')[\underline{I}-\underline{P}] - [\underline{T}(\tau_r,0)]^{(N+1)}\underline{K}(\nu')[\underline{I}-\underline{P}]e^{i\nu'(N+1)\tau_r}. \tag{52}$$

With the insertion of a factor of $\underline{P}+[\underline{I}-\underline{P}]$ before the matrix $\underline{K}(\nu')$ in the last term of (52) and use of (37) and (51), we can see that the last term in (52) vanishes as $N\to\infty$. Thus the infinite sum $\underline{S}(\nu')[\underline{I}-\underline{P}]$ in (40) may be replaced by the matrix $\underline{K}(\nu')[\underline{I}-\underline{P}]$. Using this result, we obtain

$$\tilde{g}_{\text{inc}}(\nu')=\text{Re}\,\text{tr}\left(\underline{K}(\nu')\int_0^{\tau_r}\underline{G}(\tau)e^{i\nu'\tau}d\tau\right), \tag{53}$$

where

$$\underline{G}(\tau)\equiv\frac{1}{2\tau_r}\int_0^{\tau_r}[\underline{I}-\underline{P}]\underline{T}(0,t)\underline{M}\begin{pmatrix}u_e(t)\\ v_e(t)\\ w_e(t)\\ 1\end{pmatrix} \times(1,-i,0,0)\underline{T}(t+\tau,0)dt. \tag{54}$$

Certain conclusions may now be formed about the structure of the incoherent spectrum. The ν' dependence of Eq. (53) is due to two factors—the matrix $\underline{K}(\nu')$ and the truncated Fourier transform of $\underline{G}(\tau)$. In view of the frequency-time uncertainty relation, the truncated Fourier transform is not expected to produce features narrower in frequency than $\sim 2\pi/\tau_r$. However the matrix $\underline{K}(\nu')$ can have very sharp ν' dependence if the atomic decay rate is small. This is because in the limit of small κ, the 4×4 matrix in Eq. (14) is antisymmetric and the 3×3 submatrix $\underline{T}_3$ defined by Eq. (22) therefore represents a pure rotation in 3 space. The eigenvalues of $\underline{T}_3(\tau_r,0)$ are thus 1, $e^{i\phi}$, and $e^{-i\phi}$, where ϕ is the angle of the rotation represented by $\underline{T}_3(\tau_r,0)$. Therefore $\underline{I}_3-\underline{T}_3(\tau_r,0)e^{i\nu'\tau_r}$ becomes noninvertible and $\underline{K}(\nu')$ defined by Eq. (50) blows up at triplets of frequencies ν' given by

$$\nu'-2m\pi/\tau_r=0,\ \phi/\tau_r,\ -\phi/\tau_r, \qquad m=0,\pm1,\pm2,\ldots. \tag{55}$$

Sharp peaks may therefore occur near these frequencies when κ is small but finite. That is, for $\kappa\ll|\phi|/\tau_r$, the incoherent spectrum can have fixed peaks separated from the field carrier frequency by multiples of the basic repetition frequency $2\pi/\tau_r$ and "sidebands" equally spaced on opposite sides of these fixed peaks. There is however no guarantee that a peak will occur at any particular one of these possible locations. The truncated Fourier transform of $\underline{G}(\tau)$ in Eq. (53) may be small or orthogonal to $\underline{K}(\nu')$ at a point, preventing occurrence of a peak. In the special case, treated by Mollow, of a monochromatic driving field, only a central peak and its sidebands are present in the incoherent spectrum. The absence of additional peaks is traceable to the fact that the spacing $2\pi/\tau_r$ to any additional set of peaks may be arbitrarily chosen since τ_r is arbitrary in this case.

The spacing ϕ/τ_r between a fixed peak and a sideband may be predicted in certain special cases. In the case of a monochromatic driving field, the Bloch equations describe a uniform rotation about a fixed axis at the Rabi frequency $\Omega=(\epsilon_1^2+\epsilon_2^2+\Delta\omega^2)^{1/2}$. Thus $\phi=\Omega\tau_r$ and we obtain the well-known result that the sidebands are separated from the fixed peak by the Rabi frequency Ω. Another interesting case occurs when $\epsilon_2=\Delta\omega=0$. The Bloch equations again describe a rotation about a fixed axis and ϕ may be expressed simply:

$$\phi=\int_0^{\tau_r}\epsilon_1(t)dt. \tag{56}$$

This integral is simply the pulse "area," familiar from pulse propagation studies.[9] With a pulse-train driving field of nonzero area, the separation of sidebands from fixed peaks thus varies linearly with driving field amplitude when $\Delta\omega=0$. This is highly reminiscent of the behavior in a monochromatic field. However, it should be kept in mind that as a sideband recedes from one fixed peak, it approaches the next one. Thus in contrast to the monochromatic field case, the separation between sidebands and fixed peaks can decrease as the driving amplitude is increased. Another interesting property which may be proven in the special case that $\epsilon_2=\Delta\omega=0$ is that the power spectrum is perfectly symmetric about the driving field carrier frequency ($\nu'=0$) regardless of the driving amplitude.

V. TOTAL INTENSITY

The mean total intensity of the scattered light is given by[3]

$$I_{\text{total}}(\vec{r})=\frac{1}{2\pi}\int_{-\infty}^{\infty}I(\nu,\vec{r})d\nu=\frac{1}{2\pi}|\vec{\phi}(\vec{r})|^2\int_{-\infty}^{\infty}\tilde{g}(\nu)d\nu. \tag{57}$$

Inserting (11), performing the ν' integration, and using (12c) and (13) we obtain

$$I_{\text{total}}(\vec{r})=\tfrac{1}{2}|\vec{\phi}(\vec{r})|^2\langle 1+w_e\rangle_t, \tag{58}$$

where the t-subscripted angular bracket denotes cycle averaging. Thus the mean total intensity is

proportional to the average excitation of the atom.

The coherent part of the mean intensity is obtained by inserting $\tilde{g}_{\rm coh}(\nu')$ from Eqs. (45) and (46) in place of $\tilde{g}(\nu')$ in (57) and performing the ν' integration. The result is

$$I_{\rm coh}(\vec{r}) = \tfrac{1}{4}\,|\vec{\phi}(\vec{r})|^2 \langle u_e^2 + v_e^2\rangle_t . \tag{59}$$

Thus the mean coherent intensity is proportional to the average square of the atom's dipole moment.

It is clear that at equilibrium,

$$\left\langle u\frac{du}{dt} + v\frac{dv}{dt} + w\frac{dw}{dt}\right\rangle_t = 0 .$$

Evaluating this expression using (14) we obtain a useful relationship between the components of the equilibrium Bloch vector:

$$\langle u_e^2 + v_e^2\rangle_t = -2\langle w_e(1+w_e)\rangle_t . \tag{60}$$

This formula may be used to simplify the expression for the incoherent part of the mean intensity, $I_{\rm inc}(\vec{r})$, which is obtained by subtracting (59) from (58). The result is

$$I_{\rm inc}(\vec{r}) = \tfrac{1}{2}\,|\vec{\phi}(\vec{r})|^2 \langle (1+w_e)^2\rangle_t . \tag{61}$$

Thus the mean incoherent power is proportional to the average of the square of the atomic excitation. It can be seen from (58) and (61) that in the limit of weak excitation, when $1+w$ is small, the fluorescence is almost entirely coherent.

It is interesting to note that (60) implies an upper bound to the average inversion at equilibrium:

$$\langle w_e\rangle_t \leq 0 . \tag{62}$$

This in turn imposes an upper bound on the mean total intensity given by (58):

$$I_{\rm total}(\vec{r}) \leq \tfrac{1}{2}\,|\vec{\phi}(\vec{r})|^2 . \tag{63}$$

VI. THE SPECIAL CASE OF THE TWO-MODE DRIVING FIELD

Perhaps the simplest nonconstant pulse-train envelope is that of two laser modes beating together. Specifically we write [referring to Eq. (5)]

$$\epsilon_1(t) - i\epsilon_2(t) = \epsilon_{1o} + \epsilon_{2o} e^{-i2\pi t/\tau_r} , \tag{64}$$

where ϵ_{1o} and ϵ_{2o} are the (constant) amplitudes of the two modes. Two-mode oscillation is attainable in practice[10] and has the advantage that experimentally the field envelope may be known with certainty—the relative phase is unimportant with only two modes and the observable intensity, $\epsilon_1^2 + \epsilon_2^2$ is sinusoidally modulated, with 100% modulation indicating equal intensities in the two modes.

Figure 1 shows the result of a numerical calculation of power spectra of an atom driven by the field of Eq. (64). The left-hand set of curves shows the incoherent power density $\tilde{g}_{\rm inc}(\nu')$ while the graphs on the right show the amplitudes $a_{\rm coh}(m)$ of the coherent spikes (which are in reality superimposed over the incoherent part). As noted above, the coherent spikes are located at $\nu' = 2m\pi/\tau_r$ with $m = 0, \pm1, \pm2, \ldots$. In the figure, these spikes are represented by small rectangles. The height of each rectangle represents the power in the corresponding coherent spike. The rectangles have been given a finite width such that their areas may be compared directly with areas under the peaks in the incoherent spectrum. That is, the areas on paper of the rectangles in the right-hand graphs represent the same power as similar areas under the curves in the left-hand graphs.

As can be seen from Eq. (64), the driving laser modes are located at $\nu' = 0$ and $2\pi/\tau_r$. These frequencies are indicated by small arrows on the ν' (horizontal) axes and thickened grid lines in the

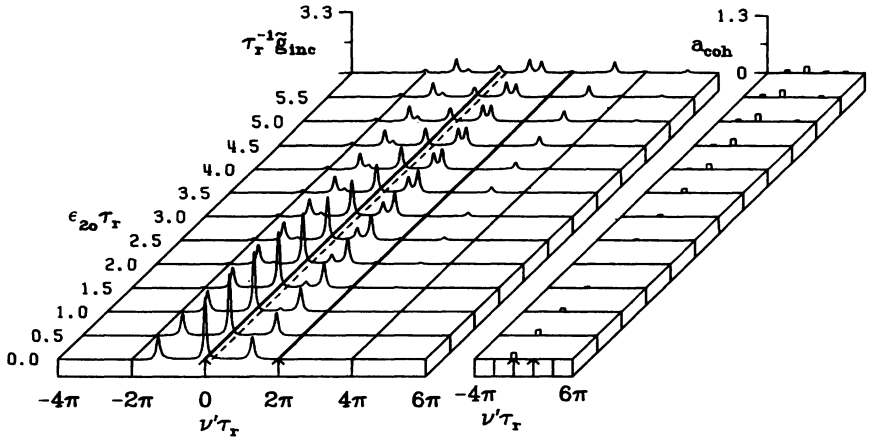

FIG. 1. Power spectra due to two-mode excitation, as the intensity of one mode is varied. The laser modes are located at $\nu' = 0$ and $2\pi/\tau_r$. Here $\epsilon_{1o} = 4.0/\tau_r$, $\Delta\omega = 0.2\,\pi/\tau_r$, and ϵ_{2o} is varied from one curve to the next. The locations of the laser modes are indicated by small arrows and thickened grid lines; $\Delta\omega$ is indicated by a dashed line.

incoherent graph. Here $\Delta\omega$, the off-resonance parameter for the atom, is fixed at $0.2\pi/\tau_r$—very near to the laser mode at $\nu'=0$, as indicated by the dashed line in the figure. Figure 1 illustrates the transition from the monochromatic driving field case treated by Mollow to a more general pulse train. The amplitude ϵ_{1_0} of the first laser mode is held fixed at $4.0/\tau_r$ while the amplitude ϵ_{2_0} of the second mode (labeled along the left) is varied from curve to curve. With $\epsilon_{2_0}=0.0$, the incoherent spectrum is the "ac Stark" triplet, familiar from Mollow's work, and the coherent part consists of a single spike. As the amplitude of the second laser mode is increased from zero, the spectra become much more complex. Additional sidebands appear and the initial symmetry is lost. The coherent spectra develop multiple spikes including spikes at frequencies other than those present in the driving field. Thus the coherent scattering is inelastic, as already mentioned.

In Figs. 2 through 4, spectra due to a driving field composed of two equal-amplitude modes are presented. We label their common amplitude by $\epsilon_0(\epsilon_0\equiv\epsilon_{1_0}\equiv\epsilon_{2_0})$. Figure 2 shows spectra resulting from symmetrical excitation. That is, $\Delta\omega$ (indicated by the dashed line) is fixed at π/τ_r—halfway between the two laser modes. The driving amplitude ϵ_0 is varied from curve to curve. The most striking feature here is the perfect symmetry about the atomic resonance frequency, regardless of the strength of the driving field. This symmetry is due to the existence of a rotating frame in which $\epsilon_2=\Delta\omega=0$. In this new rotating frame, ϵ_1 varies sinusoidally with period $2\tau_r$ and the pulse area per period defined by Eq. (56) is zero, independent of ϵ_0. Thus peaks can only occur at the fixed-peak locations, which are now at multiples of π/τ_r from the carrier frequency. This perfect symmetry and independence of peak spacing on the driving amplitude should be interesting to observe experimentally. These features will make it possible to determine exactly when the driving laser is tuned symmetrically over the atomic resonance.

In Fig. 3, the atomic resonance $\Delta\omega$, indicated by the dashed line, is fixed at $0.2\pi/\tau_r$ as in Fig. 1. Thus the atom is excited asymmetrically. For weak driving field amplitudes, the incoherent spectrum shows the characteristic "ac Stark" triplet and the coherent part shows a single spike—the atom responds linearly to the nearby mode. However, with increased driving field strength, the spectra become very complicated. The symmetry is lost, and the spacing of the peaks becomes a complicated function of intensity. We note, however, that fixed peaks still occur at frequencies ν' given by multiples of $2\pi/\tau_r$, and for fixed ϵ_0, the distances from the fixed peaks to the adjacent sidebands are all the same, as predicted in Sec. IV.

In Fig. 4, the strength of the driving field is held fixed ($\epsilon_0=4.0/\tau_r$) and the atomic resonance frequency $\Delta\omega$, shown by the dashed line, is varied in steps of $\pi/6\tau_r$ from well off-resonance ($-\pi/\tau_r$) to halfway between the two laser modes (π/τ_r). The spectrum depends on $\Delta\omega$ in a complex way and is symmetric only for $\Delta\omega=\pi/\tau_r$.

VII. SUMMARY AND CONCLUSION

We have analyzed the power spectrum of the light scattered by a two-level atom which has relaxed to equilibrium with a pulse-train driving field. The definition of the power spectrum, generalized to the case of a pulse train, is given in Eq. (9). In Eq. (30), the power spectrum is reex-

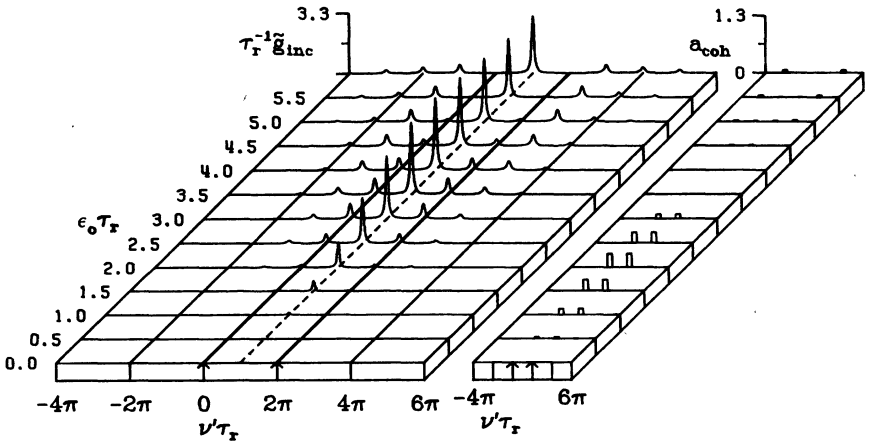

FIG. 2. Power spectra due to symmetric excitation by two equal-intensity laser modes. The driving amplitude is varied; $\Delta\omega=\pi/\tau_r$.

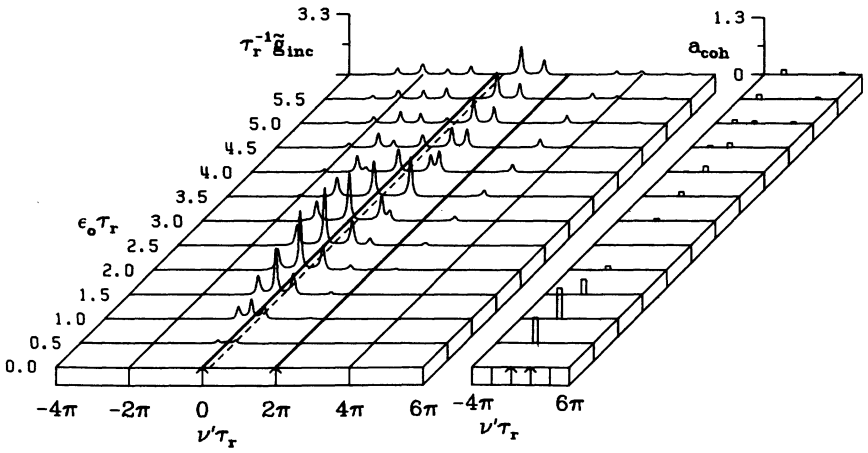

FIG. 3. Power spectra due to asymmetric excitation by two equal-intensity laser modes. The driving amplitude ϵ_o is varied; $\Delta\omega = 0.2\,\pi/\tau_r$.

pressed in terms of the solutions to the atomic Bloch equations. A projection operator for the equilibrium atomic state is defined in Eqs. (34) and (35). This operator is used to separate the coherent and incoherent components of the power spectrum [Eqs. (39) and (40)]. The final expression for the coherent part of the spectrum [Eqs. (45) and (46)] shows that this component consists of a series of spikes (delta functions) displaced from the field carrier frequency by multiples of the pulse repetition frequency. The incoherent part of the power spectrum is given in final form in Eqs. (53) and (54). With weak atomic relaxation, the incoherent spectrum has a series of peaks. Fixed peaks can occur at frequencies displaced from the field carrier by multiples of the pulse repetition frequency, and sidebands can occur equally spaced on opposite sides of these fixed peaks. Thus the peaks occur in triplets. These features are apparent in the power spectra shown in Figs. 1–4. The spectra were obtained numerically, assuming the driving field to be that of two laser modes beating together. Experimental verification of the new features predicted here will provide a test of the Mollow model of resonance fluorescence, extended to the case of a periodically varying field.

ACKNOWLEDGMENT

We wish to thank H.J. Kimble for his valuable comments and suggestions.

APPENDIX: DERIVATION OF EQ. (26)

Mollow's expression (Ref. 3, Eq. 4.6) for the atomic correlation function can be written in matrix form as

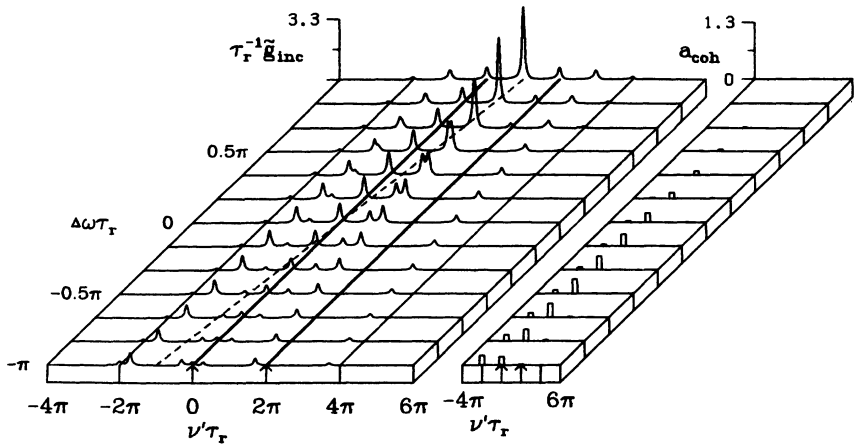

FIG. 4. Power spectra due to two equal-intensity laser modes, as the detuning ($\Delta\omega$) is varied. The driving amplitude ϵ_o is held fixed: $\epsilon_o = 4.0/\tau_r$.

$$\langle a^{\dagger}(t)a(t+\tau)\rangle = (1,0,0,0)\underline{U}(\tau;t)\underline{M}' \begin{pmatrix} \alpha(t) \\ \alpha^*(t) \\ \bar{n}(t) \\ \bar{m}(t) \end{pmatrix}, \tag{A1}$$

where $\underline{U}(\tau;t)$ is the time-translation matrix defined in Ref. 3:

$$\underline{U}(\tau;t) \equiv \begin{pmatrix} U_{\alpha\alpha} & U_{\alpha\alpha}^* & U_{\alpha\bar{n}} & U_{\alpha\bar{m}} \\ U_{\alpha^*\alpha} & U_{\alpha^*\alpha^*} & U_{\alpha^*\bar{n}} & U_{\alpha^*\bar{m}} \\ U_{\bar{n}\alpha} & U_{\bar{n}\alpha}^* & U_{\bar{n}\bar{n}} & U_{\bar{n}\bar{m}} \\ U_{\bar{m}\alpha} & U_{\bar{m}\alpha}^* & U_{\bar{m}\bar{n}} & U_{\bar{m}\bar{m}} \end{pmatrix} \tag{A2}$$

and

$$\underline{M}' \equiv \begin{pmatrix} 0 & 0 & 1 & 0 \\ 0 & 0 & 0 & 0 \\ 0 & 0 & 0 & 0 \\ 0 & 1 & 0 & 0 \end{pmatrix}. \tag{A3}$$

Equation (A1) can be rewritten as follows:

$$\langle a^{\dagger}(t)a(t+\tau)\rangle = (1,0,0,0)\underline{R}^{-1}(t+\tau)\underline{R}(t+\tau)\underline{U}(\tau;t)\underline{R}^{-1}(t)\underline{R}(t)\underline{M}'\underline{R}^{-1}(t)\underline{R}(t) \begin{pmatrix} \alpha(t) \\ \alpha^*(t) \\ \bar{n}(t) \\ \bar{m}(t) \end{pmatrix} \tag{A4}$$

where $\underline{R}(t)$ is the 4×4 transformation matrix appearing in Eq. (13) and we note that $\underline{R}^{-1}(t) = \frac{1}{2}\underline{R}^{\dagger}(t)$. Equation (26) is obtained by making the following identifications:

$$(1,0,0,0)\underline{R}^{-1}(t+\tau) = \tfrac{1}{2}e^{-i\omega(t+\tau)}(1,-i,0,0), \tag{A5}$$

$$\underline{R}(t+\tau)\underline{U}(\tau;t)\underline{R}^{-1}(t) = \underline{T}(t+\tau,t), \tag{A6}$$

$$\underline{R}(t)\underline{M}'\underline{R}^{-1}(t) = \tfrac{1}{2}e^{i\omega t}\underline{M}. \tag{A7}$$

---

[1] A readable discussion with many references may be found in the paper by C. Cohen-Tannoudji in *Proceedings of the Second Laser Spectroscopy Conference, Megève, 1975*, edited by S. Haroche, J. C. Pebay-Peyroula, T. W. Hansch, and S. H. Harris (Springer, Berlin, 1975).

[2] F. Y. Wu, R. E. Grove, and S. Ezekiel, Phys. Rev. Lett. 35, 1426 (1975); R. E. Grove, F. Y. Wu, and S. Ezekiel, Phys. Rev. A 15, 227 (1977).

[3] B. R. Mollow, Phys. Rev. 188, 1969 (1969).

[4] B. R. Mollow, Phys. Rev. A 12, 1919 (1975).

[5] M. A. Newbold and G. J. Salamo, Phys. Rev. Lett. 42, 887 (1979).

[6] L. Allen and J. H. Eberly, *Optical Resonance and Two-Level Atoms* (Wiley, New York, 1975).

[7] R. E. Slusher and H. M. Gibbs, Phys. Rev. A 5, 1634 (1972); 6, 1255 (1972).

[8] The reader who is concerned about the apparent nonconvergence of the sum in (33) may mentally replace ν' by $\nu' + i\delta$ at this point, with δ to be taken to zero at the end of the calculation. Our equations then describe the response of a detector with a frequency resolution given by δ.

[9] S. L. McCall and E. L. Hahn, Phys. Rev. 183, 457 (1969).

[10] J. A. Berry and G. J. Salamo, J. Opt. Soc. Am. 68, 1394 (1978).